JOURNAL OF WATER AND LAND DEVELOPMENT
e-ISSN 2083-4535
Polish Academy of Sciences (PAN) Institute of Technology and Life Sciences – National Research Institute (ITP – PIB)

JOURNAL OF WATER AND LAND DEVELOPMENT
DOI: 10.24425/jwld.2024.151803
2024, No. 63 (X-XII): 176–183

Examining the environmental vulnerability of the floodplain geosystem in the Syr Darya River's lower reaches

Bibatpa N. Madekesheva*[1)], Sagymbay Oketay[2)]

[1)] Eurasian National University, Department of Physical and Economic Geography, Kanysh Satbaev St 2, 010000, Astana, Kazakhstan
[2)] Al-Farabi Kazakh National University, Faculty of Geography and Environmental Management, Department of Geography, Land Management and Cadastre, 71 Al-Farabi Ave, 050040, Almaty, Kazakhstan

* Corresponding author

RECEIVED 02.06.2024 ACCEPTED 15.10.2024 AVAILABLE ONLINE 23.12.2024

Abstract: The Syr Darya River's lower reaches of floodplain geosystems face growing environmental pressures, necessitating a thorough understanding of their vulnerability on which this study focuses, emphasising the role of natural and climatic factors. The research analyses the correlations and impacts of elevation, soil density, precipitation, air temperature, and normalised difference vegetation index (*NDVI*) on environmental vulnerability. The results indicate a strong positive correlation between elevation, precipitation, air temperature, and environmental vulnerability, with *NDVI* also playing a significant role. The study employs principal components analysis to further explore these relationships and generates an integrated vulnerability map, highlighting vulnerable areas, particularly near Kyzylorda city. The map also aligns with different land cover types, emphasising the dominant influence of environmental and climatic factors, especially maximum air temperature, precipitation, and elevation, on environmental vulnerability. The research concludes that the integrated vulnerability map serves as a valuable tool for guiding environmental management and conservation strategies, enabling targeted interventions and sustainable practices in areas of high vulnerability. The study's methodology and findings offer crucial insights for effective environmental management and conservation in floodplain geosystems, promoting informed decision-making for sustainable development in the region.

Keywords: environmental vulnerability, floodplain geosystems, natural-climatic factors, principal components analysis, land cover

INTRODUCTION

The increasing growth of environmental stress and the demand for sustainable land management necessitates a thorough assessment, focusing on its impact on natural systems, including climate change (Anderson, Bayer and Edwards, 2020; Surya *et al.*, 2020). Analysing this impact on geosystems has become crucial for science-based nature management (Bychkov *et al.*, 2018; Yamashkin *et al.*, 2018; Ozgeldinova *et al.*, 2019). As integral natural and economic geosystems, river basins play a pivotal role by connecting biological, economic, and socio-demographic processes between nature and society (Henriquez-Dole *et al.*, 2018; Anchita *et al.*, 2021).

Geosystems are studied to understand the dynamic relationships between these components and how they function as an integrated whole within a particular geographical region. This holistic approach helps researchers and scientists analyse and predict changes, including the impact of human activities and environmental factors on a geosystem (Frolova, 2019; Izakovičová *et al.*, 2019).

The Syr Darya River's floodplain is a critical geosystem supporting diverse ecological and economic functions covering Central Asia (Baranovskaya, Pit'eva and Orolbaeva, 2021; Issayeva *et al.*, 2021; Zinabdin *et al.*, 2022). Its seasonal flooding creates a unique ecosystem that fosters biodiversity, including fish, birds, and other aquatic life (Kuz'mina, Shinkarenko and

Solodovnikov, 2019; Dimeyeva *et al.*, 2023). Additionally, the floodplain acts as a natural filter, improving water quality and reducing soil erosion. Furthermore, the floodplain supports agriculture, primarily for cotton, wheat, rice cultivation, and pastoralism, where livestock graze on natural grasslands and hayfields (Samarkhanov *et al.*, 2019; Baranowski *et al.*, 2020).

However, the floodplain faces threats, including climate change, overgrazing, and unsustainable land use (Rzymski *et al.*, 2019; Havrdová, Douda and Doudová, 2023). These factors result in soil degradation, biodiversity loss, and reduced water quality, making the region more vulnerable to natural disasters like floods and droughts, impacting the economy and society (Aralova, Gafurov and Toderich, 2018; Issanova *et al.*, 2022). Efficient management and conservation of the Syr Darya River's floodplain geosystems are essential for sustainable development and the region's well-being (Kuderin *et al.*, 2019). This requires an integrated, science-based approach considering ecological, economic, and social factors to promote sustainable land use practices and mitigate climate change impacts (Izakovičová *et al.*, 2019; Cherkashin, 2021).

In this regard, environmental vulnerability is an option to formulate informed decision-making in environmental management, disaster preparedness, climate adaptation, and sustainable development, ultimately contributing to the resilience of ecosystems and human communities. Common parameters used in studies for calculating environmental vulnerability typically include a combination of climatic, geographic, and ecological factors: geology, geomorphology, soil, vegetation, and land use (Choudhary, Boori and Kupriyanov, 2018). These parameters have been employed in various regions, where studies have shown strong correlations between these factors and environmental vulnerability along with social (Vieira *et al.*, 2023; Xu *et al.*, 2024). While previous studies have examined various aspects of the Syr Darya River basin, there remains a critical knowledge gap in understanding the specific environmental vulnerabilities of its floodplain geosystems, particularly in the context of the interplay between natural and climatic factors.

The study of Syr Darya River's floodplain geosystems is driven by the need for current landscape-ecological information. This information is essential for effectively managing land use through a basin-geosystem approach (Prykhodko *et al.*, 2019; Chernykh, 2022). This paper aims to comprehensively describe the state of floodplain geosystems in the Syr Darya River lowlands based on other studies where potential interrelations within the floodplain geosystem, including alterations in hydrology, soil degradation, biodiversity loss, and socioeconomic systems have been considered (Khromykh and Khromykh, 2020). The paper also identifies challenges and opportunities for sustainable land use, highlighting the geosystem's structure. Integration of parameters indicating social and natural factors through principal component analysis (PCA) and geographic information systems (GIS) allows for a comprehensive environmental vulnerability assessment across different ecosystems (Choudhary, Boori and Kupriyanov, 2018). The application of principal components analysis contributed to identifying the key natural and climatic factors driving vulnerability and developing an integrated vulnerability map, providing a valuable tool for targeted conservation efforts.

MATERIALS AND METHODS

STUDY MATERIALS

According to most authors, Syr Darya River's lowlands start from the Shardara reservoir and go down to the Kazaly irrigation zone (Asarin, Kravtsova and Mikhailov, 2010; Crétaux *et al.*, 2015; Bissenbayeva *et al.*, 2021). Based on the elevation features and hydrobasins dataset in our study, we have selected the floodplain part of the Syr Darya River's basin, starting from the eastern boundaries of the Kyzylkum desert near Turkestan city and going down to the Zhossaly city in the north-west direction according to Figure 1 (Linke *et al.*, 2019). It is a flat area with about 100–200 m elevations, the flooding zone upstream of the Syr Darya River's old delta.

In the floodplain of the Syr Darya, there are about 280 species of higher plants, some of which (*Populus pruinosa*, *Scirpus kasachstanicus*) are the habitat of species listed in the Red Book of Kazakhstan (Kaz.: Qazaqstannıñ Qızıl Kitabı) (Kuanyshova *et al.*, 2017). This area was the habitat of the Turan tiger or Caspian

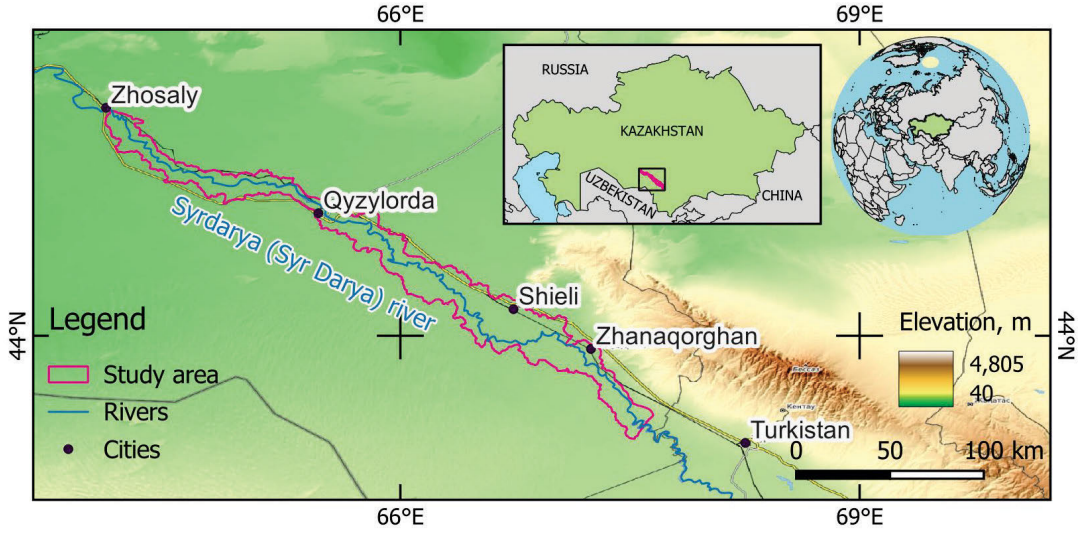

Fig. 1. The study area map; source: own study

tiger (*Panthera tigris virgata*), which was last seen here in the 1930s (Chestin *et al*., 2017). Nowadays, one of the protected relic fauna species – the Bukhara deer (*Cervus elaphus bactrianus*) that commonly used to inhabit the riparian forests till the 1960s and was re-introduced starting in 1998 within the project under the support of the World Wildlife Fund (WWF) as a part of the state program implemented by the Forestry and Wildlife Committee of the Ministry of Agriculture of the Republic of Kazakhstan (Rus.: Komitet lesnogo hozjajstva i zhivotnogo mira Ministerstva ekologii i prirodnyh resursov Respubliki Kazahstan) (WWF, 2007–2015; Pereladova, 2013).

STUDY METHODS

The study workflow (Fig. 2) was defined after establishing the study area. It consisted of three main stages: input data preparation, data analysis, overlay, and result evaluation.

Input data were clipped by area of interest and exported from the Google Earth Engine web service to analyse the floodplain geosystem's state (Amani *et al*., 2020). Our input dataset combined the elevation, median values for soil properties, vegetation, climatic data, and land cover to evaluate the state of the floodplain geosystem (Tab. 1).

NASA digital elevation model (NASADEM) is a reprocessed version of shuttle radar topography mission (SRTM) data, with the primary goal of filling voids and improving overall accuracy. It incorporates data from Advanced Spaceborne Thermal Emission and Reflection Radiometer's Global Digital Elevation Model (ASTER GDEM), Ice, Cloud, and Elevation Satellite's Geoscience Laser Altimeter System (ICESat GLAS), and Panchromatic Remote-sensing Instrument for Stereo Mapping (PRISM). While digital elevation models (DEMs) may contain errors due to land cover, the SRTM data used in this study demonstrates suitable performance (Meadows, Jones and Reinke, 2024). Notably, SRTM-derived heights over vegetated areas in North America exhibit minimal influence from forest height (Buckley *et al*., 2020). Therefore in the specific context of the Syr Darya lowlands, where tree heights range from 4 to 20 meters, the flat terrain and relatively low vegetation likely mitigate the impact of vegetation on the accuracy of elevation data (Dimeyeva *et al*., 2023). Open layer soil bulk density is a measure of soil compaction (Hengl, 2018). It reflects how tightly packed soil particles are, influencing water infiltration, root growth, and soil aeration. Open layer median monthly precipitation provides insights into the average water availability throughout the year (Hengl and Parente, 2022). Areas with low or highly variable precipitation are more susceptible to droughts, affecting agriculture, water resources, and ecosystems. Conversely, regions with excessive rainfall might face flooding and soil erosion risks. TerraClim maximum air temperature indicates the highest temperatures experienced in the area, crucial for understanding heat stress and its impacts (Abatzoglou *et al*., 2018). High maximum temperatures can exacerbate droughts, increase wildfire risks, and threaten human and ecosystem health. Vulner-

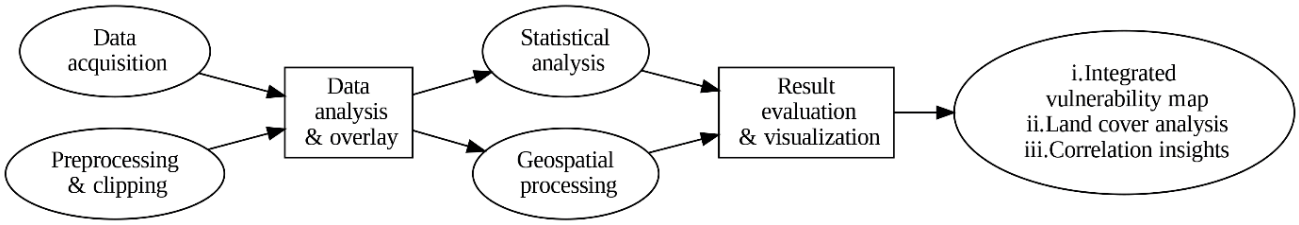

Fig. 2. The workflow of the study; source: own study

Table 1. The input dataset[1)]

No	Name	Source	Period	Description
1	NASADEM	digital elevation model (30 m)	2000	max.: 177 m, mean: 21.394 m, min.: 0 m, *SD*: 51.22 m
2	OpenLandMap	soil bulk density	1950–2018	median values at each pixel for all vertical layers (0 cm, 10 cm, 30 cm, 60 cm, 100 cm, 200 cm) were extracted; max.: 157 kg·m^{-3}, mean: 143.49 kg·m^{-3}, min.: 93 kg·m^{-3}, *SD*: 4.78 kg·m^{-3}
3	OpenLandMap	monthly precipitation	2007–2017	median monthly precipitation values at each pixel were extracted; max.: 14.58 mm, mean: 11.81 mm, min.: 9.9 mm, *SD*: 1.51 mm
4	Terra Climate	maximum air temperature	1958–2023	max.: 18.9°C, mean: 17.2°C, min.: 15.26°C, *SD*: 1.38°C
5	MOD13Q1	16-days *NDVI* dataset	2000–2024	max.: 0.45, mean: 0.25, min.: 0, *SD*: 0.07
6	Copernicus CGLS	global land cover data	2015–2019	land cover types: shrubs (class 20), herbaceous (class 30), agriculture (class 40), settlements (class 50)

[1)] The dataset covers a geographic area with a latitude ranging from approximately 43.33° to 45.47° and a longitude ranging from approximately 64.07° to 67.65°. It has a width of 13,290 pixels and a height of 7,948 pixels, providing fine spatial detail.
Explanations: NASADEM = NASA Digital Elevation Model, Copernicus CGLS = The Copernicus Global Land Service; *SD* = standard deviation, *NDVI* = normalised difference vegetation index.
Source: own study.

ability is particularly high in areas experiencing increasing temperature trends. Moderate Resolution Imaging Spectroradiometer's (MODIS) *NDVI* dataset provides a temporal view of vegetation dynamics (Didan, 2021). Low or declining *NDVI* values can indicate vegetation stress, potentially due to drought, disease, or land degradation. This information helps identify areas vulnerable to desertification, reduced agricultural productivity, and ecosystem degradation. Copernicus land cover data classifies the Earth's surface into different categories, such as forests, grasslands, and urban areas (Buchhorn *et al*., 2020). Land cover directly influences various environmental processes. For instance, forests play a vital role in regulating climate and water cycles. Conversion of natural land cover to agriculture or settlements can increase vulnerability to erosion, floods, and biodiversity loss.

The dataset layers, excluding the digital elevation model (DEM), were resampled to approximately 30 m pixel data. Then the point grid layer of over 87,000 points (the space between them is 270 m) was created to analyse possible relationships between the selected indicators from Table 1. The values of the raster were filtered using the boxplots – the statistical distribution was assessed following the exclusion of roughly 10,000 outliers. Most of the indicators possess a robust statistical foundation. Analysing their numerical values has allowed us to acquire unbiased information regarding the different factors. These indicators enable a comparative evaluation of the state of the studied geosystems. We applied the principal component analysis (PCA) technique to identify the significant indicators within the dataset and derived the principal components 1 and 2 (PC1, PC2, or PCs) (Arora *et al*., 2012) following the steps below.

a. The dataset underwent a normalisation process.
b. The covariance matrix C of the dataset was computed using the formula:

$$C = \frac{1}{n-1} X^T X \tag{1}$$

where: X = the data matrix, X^T = the transposition of matrix X, n = the number of data points.

c. Subsequently, the eigenvalues and eigenvectors of the covariance matrix were calculated.
d. The eigenvalues and their corresponding eigenvectors were then arranged in descending order of magnitude.
e. We estimated Pearson's correlation coefficient r_{xy} for elevation, soil density, precipitation, maximum air temperature, *NDVI*, population data, and PCs:

$$r_{xy} = \frac{\sum_{i=1}^{n}(x_i - \bar{x})(y_i - \bar{y})}{\sqrt{\sum_{i=1}^{n}(x_i - \bar{x})^2 \sum_{i=1}^{n}(y_i - \bar{y})^2}} \tag{2}$$

where: n = the sample size, x_i, y_i = the individual sample points indexed with i, $\bar{x}$, $\bar{y}$ = the sample means that is estimated as follows:

$$\bar{x} = \frac{1}{n}\sum_{i=1}^{n} x_i \tag{3}$$

f. To facilitate subsequent calculations, we normalised the values of the considered indicators using the following formula (Kozhokulov *et al*., 2019):

$$k = \frac{k - k_{\min}}{k_{\max} - k_{\min}} \tag{4}$$

where: k = the actual value of the indicator for a given period, $k_{\min}$ = the minimum value, $k_{\max}$ = the maximum value of the indicator.

We then reclassified the normalised values, considering the logical subsequence among natural indicators and their environmental vulnerability while factoring in climatic influences. We assigned ascending rating values, ranging from 1 to 5, to indicate environmental vulnerability (R), with 1 representing the lowest vulnerability and 5 representing the highest. Quantiles of normalised values were applied for this purpose.

After computing the statistical indicators, we calculated the environmental vulnerability of natural indicators that were used as the weighted overlay function to map the boundaries of existing geosystems utilising the formula as follows (Ashimova *et al*., 2023):

$$y = \sum_{i,j=1}^{n} w_{ij} R_{ij} \tag{5}$$

where: y = the integrated natural indicator, R_{ij} = the i-th or j-th environmental vulnerability rating, w_{ij} = the weight with which the i-th or j-th indicator contributes to the integrated indicator.

We utilise an approach based on calculating the weights of the indicators derived from pair-correlation coefficients between them to determine w_{ij}. This was performed according to the formula:

$$w_{ij} = \frac{r_{ij}}{\sum r_{ij}} \tag{6}$$

where: r_{ij} = the correlation coefficient between i-th or j-th indicator. Hence, the summation of paired correlation coefficients for each natural indicator with the others is related to the total sum of coefficients over the entire matrix of paired correlation coefficients.

After deriving the integrated natural indicator per each pixel of the study areas, we extracted its values into the point vector layer. We applied the kriging algorithm to get the smoothed map of the environmental vulnerability with clear boundaries using the system for automated geoscientific analyses (SAGA 9.2) software (Lugli *et al*., 2022). Thus, we analysed the calculated maps to describe the state of the Syr Darya River's floodplain geosystems.

RESULTS AND DISCUSSION

The dataset layers, excluding the digital elevation model (DEM), were resampled to approximately 30 m pixel data. Then, the point grid layer of over 87,000 points (the space between them was set as equal to 270 m) was created, as reported in the data and methods part of this article.

In the next step, the normalised values of each indicator were calculated for elevation, soil density, precipitation, and maximum air temperature. *NDVI* was not recalculated as it is already expressed through the coefficients, and we just filtered from 0 to 1. It resulted in the 6-dimensional array with values between 0 and 1 for further calculations (Fig. 3a).

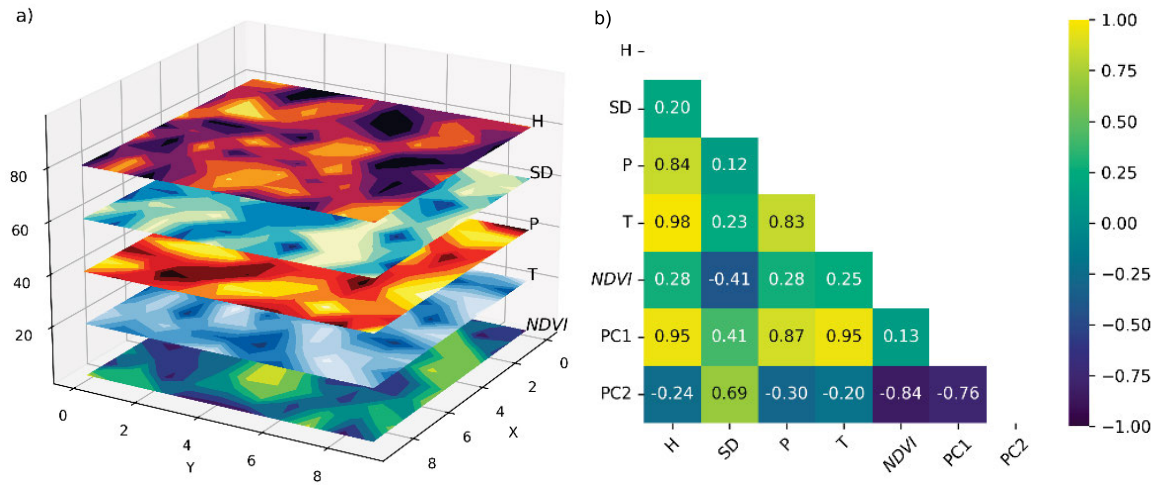

Fig. 3. Representation of: a) the raster dataset structure, b) Pearson's correlation between indicators and principal components; *H* = elevation, *SD* = soil density, *P* = precipitation, *T* = air temperature, *NDVI* = normalised difference vegetation index, source: own study

After this, the correlation coefficients were calculated by equations (1–3) from the relationships between each parameter, including principal components (PCs). It was plotted to visualise the relationships between parameters (Fig. 3b). It demonstrated that elevation, precipitation, and air temperature strongly correlate with PC1 (accordingly, 0.95, 0.87, and 0.95). We consider these the natural-climatic factors affecting the vulnerability of floodplain geosystems in the study area. In contrast, vegetation has a strong negative correlation with PC2 but still affects floodplain geosystems of the lower reaches of the Syr Darya River. That means the vegetation expressed by *NDVI* contributes to the environmental vulnerability of the study area.

The data indicates that the elevation has the highest values in the south-east (177 m) down to the north-west (about 118 m), soil density is lower in the floodplain zone of Syr Darya (down to 93 kg·m^{-3}), median monthly precipitation ranges between 10 and 15.5 mm, and maximum air temperature is between 15.3 and 19°C. The elevation patterns coincide with a maximum in the south-east and minimum to the north-west, *NDVI* has highest values in flooding zone which is in line with the soil density data and water dissemination patterns.

We normalised all the data according to Equation (4) and derived five raster data layers (elevation, soil density, *NDVI*, air temperature, precipitation) for further calculations. Then, we reclassified them to get the rating of environmental vulnerability for natural indicators (Fig. 4f). The ascending rating values, ranging from 1 to 5, to indicate environmental vulnerability are presented in Table 1 and therefore, it is a composite index derived from combination of the other factors shown in the maps of elevation (Fig. 4a), soil density (Fig. 4b), precipitation (Fig. 4c), maximum air temperature (Fig. 4d), and *NDVI* (Fig. 4e).

Environmental vulnerability ratings were considered in this order: high elevation – less vulnerable, low elevation – more vulnerable, less dense soil – highly vulnerable to soil erosion and soil salinity, high air temperature – affects most susceptible areas, along with precipitation, while *NDVI* demonstrates vegetation experiencing effects of environmental issues.

The Copernicus land cover map (Fig. 5a) and the interpolated integral environmental vulnerability map (Fig. 5b) were compared. It presents two crucial aspects of the study area along the Syr Darya River.

1. Land cover types: this map categorises the land into various types like shrubs, herbaceous areas, agriculture, and settlements. It provides the context of the landscape's composition.
2. Interpolated environmental vulnerability: this map visualises the degree of environmental vulnerability across the region, using a colour gradient ranging from low (blue) to high (red) vulnerability; the latter was prepared to delineate vulnerability level boundaries by applying the kriging algorithm.

We could see that most of the area is occupied by herbaceous vegetation (almost 50%) and agriculture (29%), followed by shrubs (9%) and settlements (2%). Other land cover types were not included. Then, the most vulnerable areas were detected south of Kyzylorda city, close to the Kyzylkum Desert, which has low precipitation and high temperatures. There are large, abandoned areas of croplands near that city, which aligns with this study's findings (Löw *et al.*, 2018). They reported that most of the abandoned agricultural land was concentrated in Kazakhstan, accounting for 38% of the total cropland abandonment in the Aral Sea region. Among these regions, Kyzyl-Orda in Kazakhstan had the highest percentage of abandoned cropland, reaching 49%.

Abandoned croplands represent a significant land cover change that can directly impact environmental vulnerability. These areas are susceptible to further degradation, affecting soil health, water resources, and biodiversity. Recognising this connection is crucial for understanding the dynamic nature of vulnerability in the region.

Identifying large, abandoned croplands also points towards potential opportunities for restoration and sustainable land management. These areas could be targeted for reforestation, agroforestry, or other practices that enhance ecosystem services and reduce vulnerability.

Figure 5b illustrates the spatial distribution of environmental vulnerability in the study region. The area south of Kyzylorda is particularly vulnerable due to a combination of its proximity to the arid desert, susceptible land cover types, and potential human pressures. This information is crucial for prioritising conservation efforts and sustainable land management practices in the region.

The areas with a significant concentration of abandoned cropland were primarily found in the lower-lying regions of

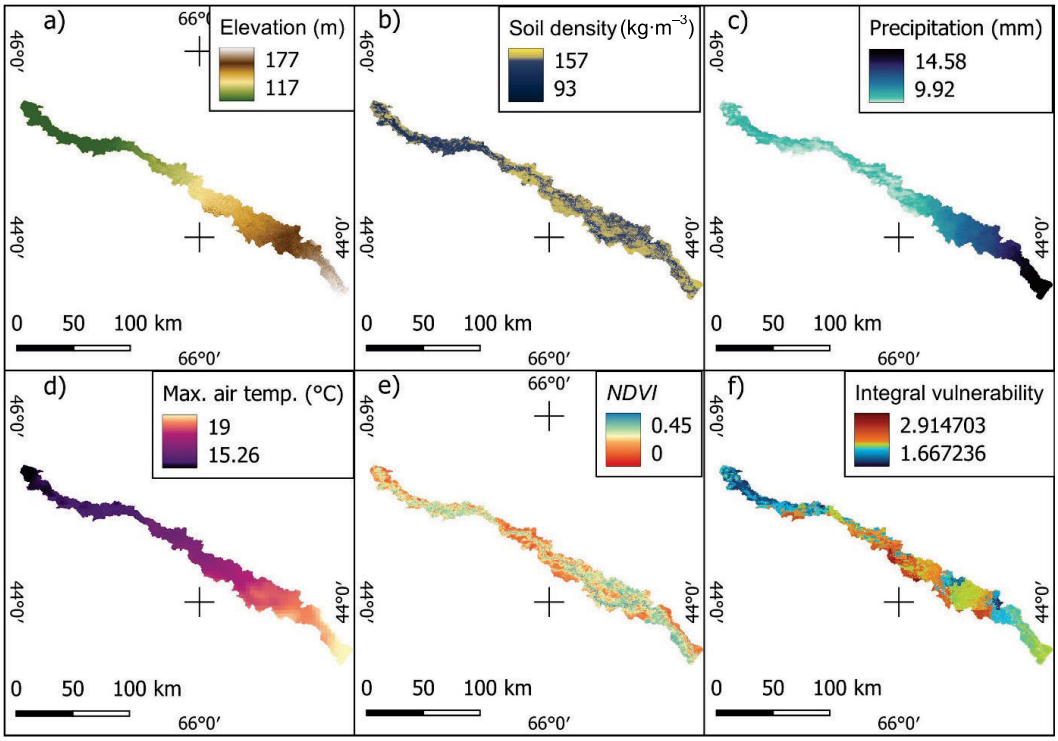

Fig. 4. Raster data layers: a) elevation, b) soil density, c) precipitation, d) maximum air temperature, e) normalised difference vegetation index (*NDVI*), f) integral vulnerability; source: own study

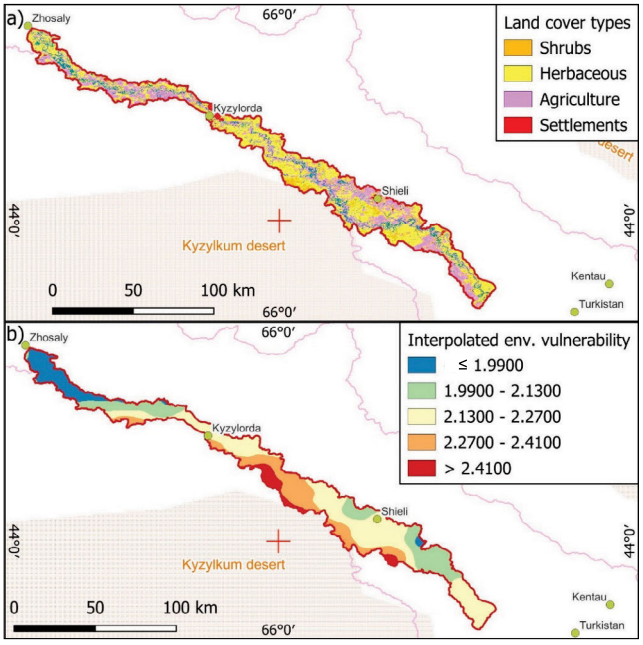

Fig. 5. Maps of the study area: a) land cover map (Copernicus GLCS), b) the integrated environmental vulnerability; source: own study

Kazakhstan, such as Kazalinsk and Kyzyl-Orda. Cropland abandonment was prevalent in Kyzyl-Orda with moderate to excellent suitability for wheat cultivation, a similar pattern for rice production, and varying suitability from high to very high. Therefore, identifying and understanding the vulnerability of abandoned croplands is crucial for developing sustainable land management strategies and prioritising restoration efforts in the region.

Considering the principal components, we revealed that they include maximum air temperature, precipitation, and elevation, which are mutually correlated. Therefore, we can state that environmental-climatic factors are the primary cause of major environmental vulnerability.

CONCLUSIONS

The study comprehensively evaluates the environmental vulnerability of floodplain geosystems in the Syr Darya River's lower reaches, underscoring the critical role of natural and climatic factors. By integrating diverse datasets and employing principal components analysis, the research identified key vulnerability drivers and resulted in an integrated vulnerability map, which serves as a valuable tool for guiding targeted conservation efforts and sustainable land management practices. The findings highlight the dominant influence of maximum air temperature, precipitation, and elevation on environmental vulnerability, particularly in areas near Kyzylorda city, aligning with abandoned croplands. The methodological framework presented in this study can be adapted and applied to other floodplain environments, facilitating a broader understanding of environmental vulnerability and informing effective conservation strategies in similar contexts.

The research outcomes contribute significantly to environmental management and conservation by providing a detailed understanding of the factors influencing vulnerability in floodplain geosystems. The integrated vulnerability map, a key output of this study, offers a practical tool for decision-makers and stakeholders to prioritise conservation efforts and implement sustainable land management practices in the most vulnerable areas. Though digital elevation model (DEM) has its limitations, the identification of maximum air temperature, precipitation, and elevation as primary vulnerability drivers underscores the urgent need to address climate change impacts and apply an adaptive management

strategies in the region. The methodological approach employed in this study, combining geospatial analysis and statistical techniques, can be readily transferred to other floodplain environments, enabling researchers and practitioners to assess and address environmental vulnerabilities in diverse contexts.

Future research can build upon these findings by incorporating additional factors, such as socioeconomic variables and land-use practices, to develop more nuanced vulnerability assessments and support sustainable development initiatives in floodplain regions. Integration of these factors would provide a more holistic understanding of the complex interactions between human activities and environmental processes, enabling the formulation of comprehensive and effective conservation strategies. Furthermore, future studies can explore the temporal dynamics of environmental vulnerability in floodplain geosystems, considering the potential impacts of climate change and other anthropogenic pressures on the long-term sustainability of these vital ecosystems. The insights gained from such research will be instrumental in guiding adaptive management approaches and ensuring the resilience of floodplain environments in the face of ongoing global change.

ACKNOWLEDGEMENTS

We are immensely grateful to the staff and colleagues at the Eurasian National University and The Bobek International Scientific Research Institute for their invaluable insights and expertise, which greatly assisted the research. Their perspectives and suggestions were helpful.

Additionally, we would like to acknowledge the contributions of various experts and researchers whose published works provided foundational understanding and guidance. Their extensive knowledge and prior findings were crucial in shaping the direction and scope of our study.

Our thanks also go to the team at Google Earth Engine for providing access to vital data sets and tools that enriched our analysis. Their platform was indispensable for the spatial analysis conducted in our study.

FUNDING

The study was funded by the Ministry of Science and Higher Education grant in 2016–2019, which L.N. Gumilyov National State University managed.

CONFLICT OF INTERESTS

All authors declare that they have no conflict of interests.

REFERENCES

Abatzoglou, J.T. *et al.* (2018) "TerraClimate, a high-resolution global dataset of monthly climate and climatic water balance from 1958–2015," *Scientific Data*, 5(1). Available at: https://doi.org/10.1038/sdata.2017.191.

Amani, M. *et al.* (2020) "Google Earth Engine Cloud computing platform for remote sensing big data Applications: A comprehensive review," *IEEE Journal of Selected Topics in Applied Earth Observations and Remote Sensing*, 13, pp. 5326–5350. Available at: https://doi.org/10.1109/jstars.2020.3021052.

Anchita, *et al.* (2021) "Health impact of drying Aral Sea: One health and socio-economical approach," *Water*, 13(22), 3196. Available at: https://doi.org/10.3390/w13223196.

Anderson, R., Bayer, P.E. and Edwards, D. (2020) "Climate change and the need for agricultural adaptation," *Current Opinion in Plant Biology*, 56, pp. 197–202. Available at: https://doi.org/10.1016/j.pbi.2019.12.006.

Aralova, D., Gafurov, D. and Toderich, K. (2018) "NDVI-based monitoring long-term vegetation change dynamics in the drylands of Central Asia," in D. Egamberdieva, M. Öztürk (eds.) *Vegetation of Central Asia and Environs*. Cham: Springer, pp. 49–71. Available at: https://doi.org/10.1007/978-3-319-99728-5_3.

Arora, R. *et al.* (2012) "Stochastic optimization for PCA and PLS," *50th Annual Allerton Conference on Communication, Control, and Computing (Allerton)*, pp. 861–868. Available at: https://doi.org/10.1109/allerton.2012.6483308.

Asarin, A.E., Kravtsova, V.I. and Mikhailov, V.N. (2010) "Amudarya and Syrdarya rivers and their deltas," in A.G. Kostianoy, A.N. Kosarev (eds.) *The Aral Sea environment*. Berlin–Heidelberg: Springer. pp. 101–121. Available at: https://doi.org/10.1007/698_2009_8.

Ashimova, B. *et al.* (2023) "Environmental hazards of the railway infrastructure of Kazakhstan," *Sustainability*, 15(2), 1321. Available at: https://doi.org/10.3390/su15021321.

Baranovskaya, E.I., Pit'eva, K.E. and Orolbaeva, L.E. (2021) "Conditions for forming groundwater in artesian basins of the intermountain type," *Moscow University Geology Bulletin*, 76(5), pp. 578–588. Available at: https://doi.org/10.3103/s0145875221050045.

Baranowski, E. *et al.* (2020) "Pastoral farming in the Ili Delta, Kazakhstan, under decreasing water inflow: An economic assessment," *Agriculture*, 10(7), 281. Available at: https://doi.org/10.3390/agriculture10070281.

Bissenbayeva, S. *et al.* (2021) "Long-term variations in runoff of the Syr Darya River Basin under climate change and human activities," *Journal of Arid Land*, 13(1), pp. 56–70. Available at: https://doi.org/10.1007/s40333-021-0050-0.

Buchhorn, M. *et al.* (2020) "Copernicus global land cover layers–Collection 2," *Remote Sensing*, 12(6), 1044. Available at: https://doi.org/10.3390/rs12061044.

Buckley, S.M. *et al.* (2020) *NASADEM*. Pasadena: National Aeronautics and Space Administration Jet Propulsion Laboratory California Institute of Technology. https://lpdaac.usgs.gov/documents/592/NASADEM_User_Guide_V1.pdf (Accessed: April 18, 2024).

Bychkov, I.V. *et al.* (2018) "Water protection zoning as an instrument of preservation for Lake Baikal," *Water*, 10(10), 1474. Available at: https://doi.org/10.3390/w10101474.

Cherkashin, A.K. (2021) "Geosystems and the geographical environment," *Geography and Natural Resources*, 42(1), pp. 1–9. Available at: https://doi.org/10.1134/s1875372821010066.

Chernykh, D. (2022) "Basin approach as a tool for landscape assessment and planning," *Current Landscape Ecology Reports*, 7(2), pp. 15–23. Available at: https://doi.org/10.1007/s40823-022-00069-4.

Chestin, I.E. *et al.* (2017) "Tiger re-establishment potential to former Caspian tiger (*Panthera tigris virgata*) range in Central Asia," *Biological Conservation*, 205, pp. 42–51. Available at: https://doi.org/10.1016/j.biocon.2016.11.014.

Choudhary, K., Boori, M.S. and Kupriyanov, A. (2018) "Spatial modelling for natural and environmental vulnerability through

remote sensing and GIS in Astrakhan, Russia," *The Egyptian Journal of Remote Sensing and Space Science*, 21(2), pp. 139–147. Available at: https://doi.org/10.1016/j.ejrs.2017.05.003.

Crétaux, J.-F. *et al.* (2015) "Global surveys of reservoirs and lakes from satellites and regional application to the Syrdarya river basin," *Environmental Research Letters*, 10(1), 015002. Available at: https://doi.org/10.1088/1748-9326/10/1/015002.

Dimeyeva, L. *et al.* (2023) "Plant diversity and distribution patterns of *Populus pruinosa* Schrenk (Salicaceae) floodplain forests in Kazakhstan," *Diversity*, 15(7), 797. Available at: https://doi.org/10.3390/d15070797.

Didan, K. (2021) *MODIS/Terra Vegetation Indices 16-Day L3 Global 250m SIN Grid V061*. NASA EOSDIS Land Processes Distributed Active Archive Center. Available at: https://doi.org/10.5067/MODIS/MOD13Q1.061.

Frolova, M. (2019) "From the Russian/Soviet landscape concept to the geosystem approach to integrative environmental studies in an international context," *Landscape Ecology*, 34(7), pp. 1485–1502. Available at: https://doi.org/10.1007/s10980-018-0751-8.

Havrdová, A., Douda, J. and Doudová, J. (2023) "Threats, biodiversity drivers and restoration in temperate floodplain forests related to spatial scales," *Science of The Total Environment*, 854, 158743. Available at: https://doi.org/10.1016/j.scitotenv.2022.158743.

Hengl, T. (2018) "Soil bulk density (fine earth) 10 x kg/m-cubic at 6 standard depths (0, 10, 30, 60, 100 and 200 cm) at 250 m resolution. Data set (v02)," *Zenodo*. Available at: https://doi.org/10.5281/zenodo.2525665.

Hengl, T. and Parente, L. (2022) "Open monthly precipitation in mm at 1 km resolution (multisource average) based on SM2RAIN-ASCAT 2007-2021, CHELSA Climate and WorldClim. Data set," *Zenodo*. Available at: https://doi.org/10.5281/zenodo.6458580.

Henríquez-Dole, L. *et al.* (2018) "Integrating strategic land use planning in the construction of future land use scenarios and its performance: The Maipo River Basin, Chile," *Land Use Policy*, 78, pp. 353–366. Available at: https://doi.org/10.1016/j.landusepol.2018.06.045.

Issanova, G. *et al.* (2022) "Soil salinisation as a land degradation process in the dried bed of the North-eastern Aral Sea, Kazakhstan," *Arabian Journal of Geosciences*, 15, 1055. Available at: https://doi.org/10.1007/s12517-022-09627-w.

Issayeva, A. *et al.* (2021) "Comparative assessment of geomorphological and landscape features around the Small Aral Sea," *Journal of Ecological Engineering*, 22(10), pp. 73–84. Available at: https://doi.org/10.12911/22998993/142187.

Izakovičová, Z. *et al.* (2019) "The integrated approach to landscape management – Experience from Slovakia," *Sustainability*, 11(17), 4554. Available at: https://doi.org/10.3390/su11174554.

Khromykh, V.V. and Khromykh, O.V. (2020) "GIS-based study of landscape structure and land use within the river valleys in the Southern Tomsk Region: Spatial-temporal aspects," in A.V. Khoroshev, K.N. Dyakonov (eds.) *Landscape patterns in a range of spatio-temporal scales*, pp. 405–420. Available at: https://doi.org/10.1007/978-3-030-31185-8_25.

Kozhokulov, S. *et al.* (2019) "Assessment of tourism impact on the socio-economic spheres of the Issyk-Kul Region (Kyrgyzstan)," *Sustainability*, 11(14), 3886. Available at: https://doi.org/10.3390/su11143886.

Kuanyshova, S.E. *et al.* (2017) "Bioraznoobraziye flory poymy i del'ty reki Syrdar'i [Flora biodiversity in flood plain and delta of the Syrdarya River]," *Nauka i mir*, 4(44), pp. 10–14. Available at: https://scienceph.ru/f/science_and_world_no_4_44_april_vol_ii.pdf (Accessed: April 14, 2023).

Kuderin, A. *et al.* (2019) "Landscape planning of the Kazaly irrigation array of Southern Kazakhstan," *European Journal of Geography*, 10(1) Available at: https://www.eurogeojournal.eu/index.php/egj/article/view/61 (Accessed: July 22, 2023).

Kuz'mina, Zh.V., Shinkarenko, S.S. and Solodovnikov, D.A. (2019) "Main tendencies in the dynamics of floodplain ecosystems and landscapes of the lower reaches of the Syr Darya River under modern changing conditions," *Arid Ecosystems*, 9(4), pp. 226–236. Available at: https://doi.org/10.1134/s207909611904005x.

Linke, S. *et al.* (2019) "Global hydro-environmental sub-basin and river reach characteristics at high spatial resolution," *Scientific Data*, 6(1). Available at: https://doi.org/10.1038/s41597-019-0300-6.

Löw, F. *et al.* (2018) "Mapping cropland abandonment in the Aral Sea Basin with MODIS time series," *Remote Sensing*, 10(2), 159. Available at: https://doi.org/10.3390/rs10020159.

Lugli, F. (2021) "A strontium isoscape of Italy for provenance studies," *Chemical Geology*, 587, 120624. Available at: https://doi.org/10.1016/j.chemgeo.2021.120624.

Meadows, M., Jones, S. and Reinke, K. (2024) "Vertical accuracy assessment of freely available global DEMs (FABDEM, Copernicus DEM, NASADEM, AW3D30 and SRTM) in flood-prone environments," *International Journal of Digital Earth*, 17(1). Available at: https://doi.org/10.1080/17538947.2024.2308734.

Ozgeldinova, Z.O. *et al.* (2019) "Assessment of human impacts on geosystems of Sarysu River basin," *Fresenius Environmental Bulletin*, 28(8), pp. 6019–6026.

Pereladova, O. (2013) "Restoration of Bukhara deer (*Cervus elaphus bactrianus* Lydd.) in Central Asia in 2000-2011," *Deer Specialist Group Newsletter*, 25, pp. 19–30.

Prykhodko, M.M. *et al.* (2019) "Application of the geographic information system technologies in the geosystem planning process," in *18th International Conference on Geoinformatics – Theoretical and Applied Aspects*. Kyiv, Ukraine 13–16 May 2019, pp. 1–5. Kyiv: European Association of Geoscientists & Engineers.

Rzymski, P. *et al.* (2019) "Pollution with trace elements and rare-earth metals in the lower course of Syr Darya River and Small Aral Sea, Kazakhstan," *Chemosphere*, 234, pp. 81–88. Available at: https://doi.org/10.1016/j.chemosphere.2019.06.036.

Samarkhanov, K. *et al.* (2019) "The spatial and temporal land cover patterns of the Qazaly irrigation zone in 2003–2018: The case of Syrdarya River's lower reaches, Kazakhstan," *Sustainability*, 11(15), p. 4035. Available at: https://doi.org/10.3390/su11154035.

Surya, B. *et al.* (2020) "Land use change, spatial interaction, and sustainable development in the metropolitan urban areas, South Sulawesi Province, Indonesia," *Land*, 9(3), 95. Available at: https://doi.org/10.3390/land9030095.

Vieira, R.M.S.P. *et al.* (2023) "Socio-environmental vulnerability to drought conditions and land degradation: An assessment in two northeastern Brazilian river basins," *Sustainability*, 15(10), 8029. Available at: https://doi.org/10.3390/su15108029.

WWF (2007–2015) *Biodiversity preservation and integrated river basin development in the Syrdaria River Valley. Project start date: 2007 – End date: 2015*. World Wildlife Fund.

Xu, C. *et al.* (2024) "Spatiotemporal variations of eco-environmental vulnerability in Shiyang River Basin, China," *Ecological Indicators*, 158, 111327. Available at: https://doi.org/10.1016/j.ecolind.2023.111327.

Yamashkin, S. *et al.* (2018) "Using ensemble systems to study natural processes," *Journal of Hydroinformatics*, 20(4), pp. 753–765. Available at: https://doi.org/10.2166/hydro.2018.076.